

Optothermal Properties of Fibers. X. Temperature Dependence of the Skin–Core Structure of Nylon-6 Fibers

I. M. FOUDA,¹ M. M. EL-TONSY,¹ H. M. HOSNY,² F. M. METAWE,³ K. H. EASAWI³

¹ Physics Department, Faculty of Science, Mansoura University, Mansoura, Egypt

² Physics Department, Faculty of Science, Ain Shams University, Ain Sham, Egypt

³ Mathematical and Natural Science Department, Faculty of Engineering, Shoubra, Benha Branch, Zagazig University, Zagazig, Egypt

Received 8 November 1996; accepted 3 April 1997

ABSTRACT: Refractive indices and birefringence for skin and core changes with annealing, produced by different annealing conditions in nylon-6 fibers, were measured interferometrically. Applications were carried out using multiple-beam Fizeau fringes in transmission to determine Cauchy's constants and dispersive coefficients for the fibers. The resulting data were used to calculate the polarizability per unit volume for each layer. By optical microscopy, the geometrical parameters of the fiber cross section were found. The effect of temperature and time of annealing on the refractive index and birefringence for each layer were also investigated. The relationships between temperature and time of annealing with the optical parameters were drawn. Illustrations are given using microinterferograms and curves. © 1997 John Wiley & Sons, Inc. *J Appl Polym Sci* **66**: 695–709, 1997

INTRODUCTION

The study of optical anisotropy in polymer fibers plays an important role in the knowledge of the molecular arrangement within these fibers.¹ Double refraction or birefringence depends on the molecular orientation in polymer fibers as it contains contributions from the polarizabilities of all molecular units in the sample.² The structure of these fibers can be characterized on the molecular level by determining their refractive indices and birefringence of each layer of the fiber.

Recently, application of double-beam and multiple-beam Fizeau fringes interferometry has

stimulated interest in studying the effect of different types of chemical, mechanical, and thermal properties of natural and man-made fibers.^{3–9} The most available technique for changing the polymeric structure is the annealing and quenching process.^{10–15} The effects of annealing increased drastically with temperature, so thermal treatment was used to vary the degree of crystallinity in polymeric materials.

Annealing may be performed with the ends of the sample free or fixed. In the former case, the sample shrunk, whereas in the latter case, it retained its length but exerted measurable retractive forces on its fixed ends. Both effects were increased with increased annealing temperature.

In the present work, the changes in the optical parameters of nylon-6 fibers due to the annealing processes were determined interferometrically. Multiple-beam Fizeau fringes were used for the de-

Correspondence to: I. M. Fouda.

Journal of Applied Polymer Science, Vol. 66, 695–709 (1997)

© 1997 John Wiley & Sons, Inc.

CCC 0021-8995/97/040695-15

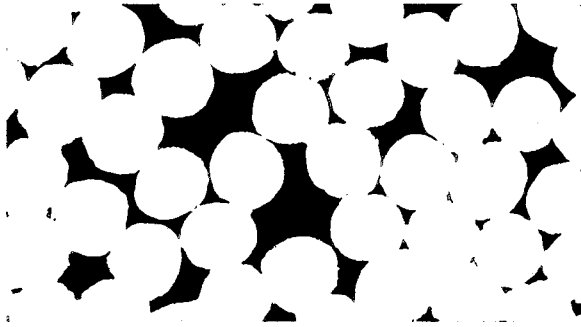


Plate 1 Optical cross section of unannealed nylon-6 fibers.

termination of the mean, skin, and core refractive indices (n_a^{\parallel} , n_a^{\perp} , n_s^{\parallel} , n_s^{\perp} , n_c^{\parallel} , and n_c^{\perp}) and also the birefringence in each case for nylon-6 fibers with different annealing conditions (Δn_a , Δn_s , and Δn_c).

THEORETICAL CONSIDERATIONS

Interferometric Measurement of the Optical Parameters

Multiple-beam Fizeau fringes in transmission were used for the determination of the optical parameters for annealed nylon-6 fibers.

Determination of Refractive Indices and Birefringence for the Nylon-6 Fiber Layers

Nylon-6 Fibers with Circular Cross Section and Having Skin-Core Layers. In the present work, we determined the refractive indices and birefringence of unannealed and annealed nylon-

6 fibers with multilayers of skin by applying the following equation¹⁶:

$$\frac{dz}{h} = \frac{4}{\lambda} \sum_{J=0}^i A_J \quad (1)$$

where $A_J = (n_J - n_{J+1})(r_J^2 - x^2)^{1/2} r_J$ is the radius of the skin of order J from the core; λ , the wavelength of monochromatic light used; and dz , the value of the fringe shift. h is the fraction of an order separation between two consecutive straight-line fringes at the same point from the center of the fiber, while x is the distance measured from the center of the fringe shift and at which the fringe shift tends to zero. Hence,

$$n_L = n_{i+1}, \quad n_0 = n_c \quad \text{and} \quad r_i = r_f, \quad r_0 = r_c$$

where n_0 is the refractive index of the central layer of the fiber (the core); r_f , the radius of the whole fiber; and r_c , the radius of the core.

The Mean Refractive Index n_a . The mean refractive index n_a of the nylon-6 fibers, having a core of radius r_c and a refractive index n_c surrounded by a skin layer of thickness r_s and refractive index n_s , is calculated using the following formula¹⁷:

$$n_a = \frac{r_s}{r_f} \cdot n_s + \frac{r_c}{r_f} \cdot n_c \quad (2)$$

Measurement of the Diameter of Nylon-6 Fibers by Optical Microscopy

The optical technique was used in determining the cross section of the unannealed fibers. The optical cross sections of unannealed

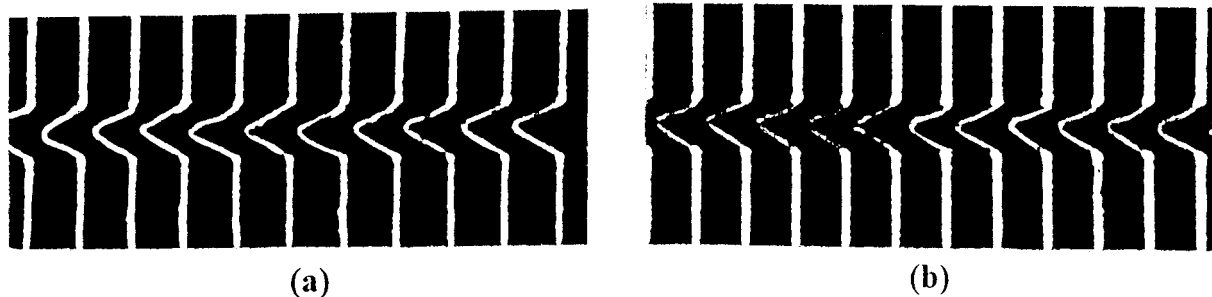


Plate 2 Microinterferograms of multiple-beam Fizeau fringes in transmission of nylon-6 fibers using monochromatic light of wavelength $\lambda = 546.1$ nm vibrating perpendicular to the fiber axis: (a) unannealed fiber; (b) annealed for 5 h at 90°C.

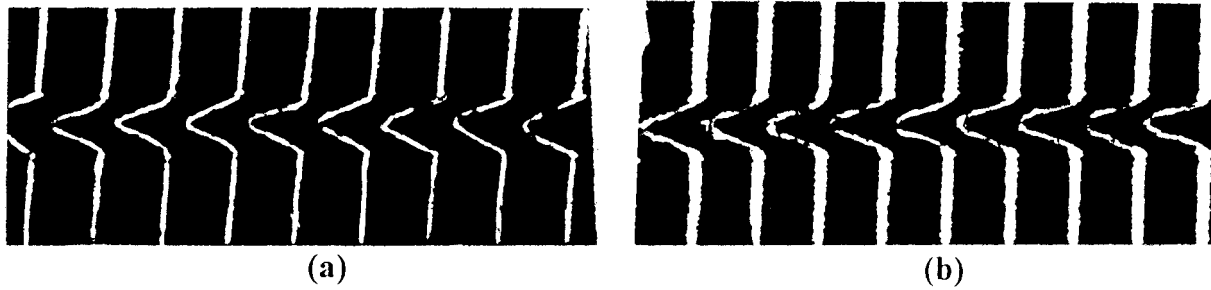


Plate 3 Microinterferograms of multiple-beam Fizeau fringes in transmission of nylon-6 fibers using monochromatic light of wavelength $\lambda = 546.1$ nm vibrating parallel to the fiber axis: (a) unannealed fiber; (b) annealed for 5 h at 90°C .

nylon-6 fibers are shown in Plate 1, which shows a perfectly circular shape with diameters of about 19.8 microns with an error of ± 0.3 micron. The mean cross-sectional area was about $3.079 \times 10^{-10} \text{ m}^2$.

Annealing of Samples

Long bundles of nylon-6 fibers were loosely folded in a cocoon form with both ends free.

Several samples, placed in special small glass bottles, were heated in an oven (Model WT, binder type E53, Germany) at constant temperature. The temperatures ranged from 90 to 175°C with an error of $\pm 2^{\circ}\text{C}$ for different annealing times, ranging from 1 to 10 h. The samples were then left to cool in the oven to room temperature (27°C) with an error of $\pm 1^{\circ}\text{C}$. Hence, for each annealing temperature,

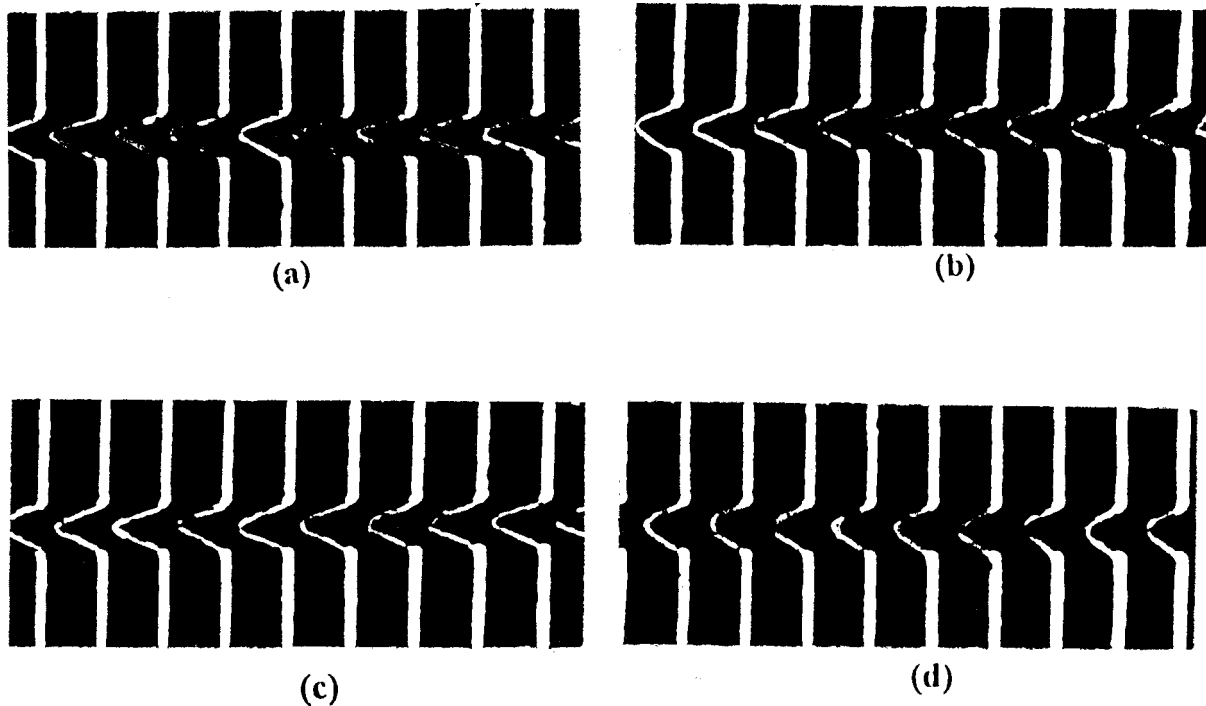


Plate 4 Microinterferograms of multiple-beam Fizeau fringes in transmission of nylon-6 fibers using monochromatic light of wavelength $\lambda = 546.1$ nm vibrating perpendicular to the fiber axis. The fiber was annealed for 3 h at (a) 90°C , (b) 110°C , (c) 125°C , and (d) 155°C .

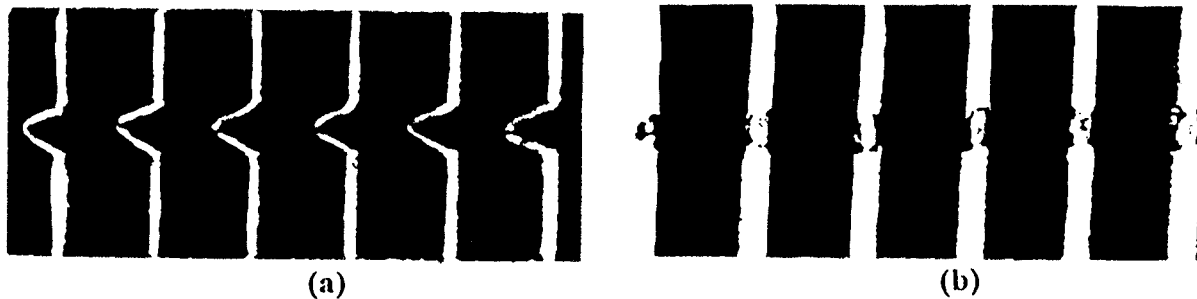


Plate 5 Microinterferograms of multiple-beam Fizeau fringes in transmission of nylon-6 fibers using monochromatic light of wavelength $\lambda = 546.1$ nm vibrating parallel to the fiber axis. The fiber was annealed for 3 h at (a) 125°C and (b) 155°C.

10 samples were annealed at different durations.

INTERFEROMETRIC MEASUREMENTS OF THE OPTICAL PARAMETERS

Multiple-Beam Fizeau Fringes in Transmission for Determining the Skin, Core, and Mean Refractive Indices and the Birefringences of Nylon-6 Fibers

The multiple-beam Fizeau fringes in the transmission method was used for determining the optical parameters of the skin, core, and mean refractive indices, namely, n_s^{\parallel} , n_s^{\perp} , n_c^{\parallel} , n_c^{\perp} , n_a^{\parallel} , and n_a^{\perp} . The skin, core, and mean birefringences, Δn_s , Δn_c , and Δn_a , were also calculated.

These values were determined for several samples of nylon-6 fibers annealed at different temperatures: 90, 110, 125, 140, 155, 165, and 175°C, for the constant time intervals of 3 and 5 h. Other samples of nylon-6 fibers, annealed for different intervals of time (1–10 h) at the constant annealing temperature of 140°C, were examined by the same technique. Throughout this experiment, the green line of a mercury lamp of wavelength $\lambda = 546.1$ nm was used.

Plate 2a is a microinterferogram of multiple-beam Fizeau fringes in the transmission of an unannealed nylon-6 fiber, whereas Plate 2b is a microinterferogram of multiple-beam Fizeau fringes in the transmission of an annealed fiber for a constant time of 5 h at the annealing temperature of 90°C. The refractive index of the used immersion liquid for the perpendicular component of the fiber was 1.5397 at 27°C.

The microinterferogram of multiple-beam Fizeau fringes in the transmission of an un-

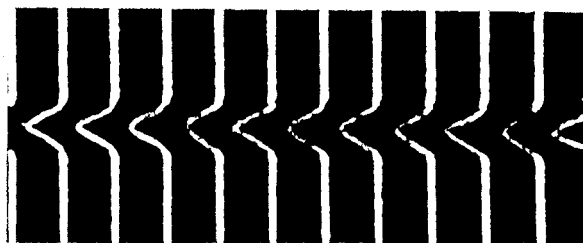
annealed nylon-6 fiber is shown in Plate 3a. The microinterferogram of multiple-beam Fizeau fringes in the transmission shown in Plate 3b corresponds to the fiber annealed for the constant time of 5 h at the annealing temperature of 90°C. The refractive index of the used immersion liquid for the parallel component of the fiber was 1.5884 at 27°C.

Plate 4(a)–(d) are microinterferograms of multiple-beam Fizeau fringes in the transmission of annealed nylon-6 fibers for a constant time of 3 h at different annealing temperatures: 90, 110, 125, and 155°C, respectively. The refractive index of the used immersion liquid for the perpendicular component of the fiber was 1.5393 at 27°C.

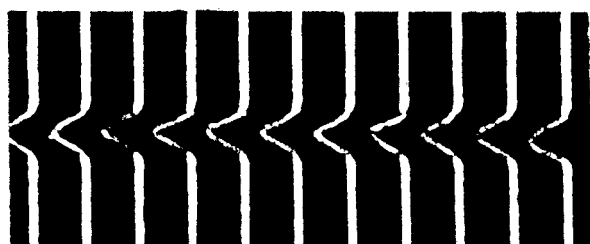
The microinterferograms of nylon-6 fibers annealed for 3 h at different annealing temperatures, 125 and 155°C, respectively, are shown in Plate 5(a) and (b). The refractive index of the used immersion liquid for the parallel component of the fiber was 1.5878 at 27°C.

Plate 6(a)–(c) are microinterferograms of multiple-beam Fizeau fringes in the transmission corresponding to nylon-6 fibers annealed at a constant temperature of 140°C for different intervals of time: 1, 2, and 3 h, respectively. The refractive index of the used immersion liquid for the perpendicular component was 1.5397 at 27°C.

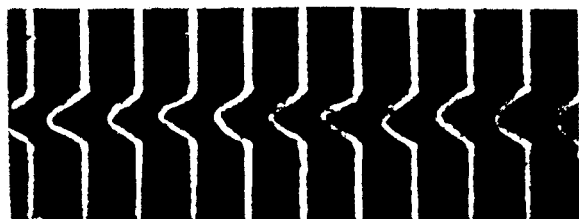
The values of the fringe shift for the parallel component of the fiber skin dz_s^{\parallel} , of the fiber core dz_c^{\parallel} and the interfering spacing h were measured from the microinterferograms. The thickness of the skin r_s and the radius of the core r_c were also obtained from the microinterferograms. The radius of the fiber r_f was deduced from both the microinterferograms and from the obtained optical cross section (Plate 1).



(a)



(b)



(c)

Plate 6 Microinterferograms of multiple-beam Fizeau fringes in transmission of nylon-6 fibers using monochromatic light of wavelength $\lambda = 546.1$ nm vibrating perpendicular to the fiber axis. The fiber was annealed at 140°C for (a) 1 h, (b) 2 h, and (c) 3 h.

The fringe shift of the fiber in Plates 2–6 was found to be away from the apex of the interferometer. This indicated that, for the perpendicular and parallel components, the refractive index of the selected liquid was higher than that of the fiber. It was observed from Plates 2–6 that as the annealing temperatures and time were increased the fringe shift decreased, i.e., the refractive index of the annealed fiber increased with increase of the annealing temperatures and time intervals. By using eq. (1), the skin, n_s^{\parallel} , and core, n_c^{\parallel} , refractive indices were calculated; from a similar for-

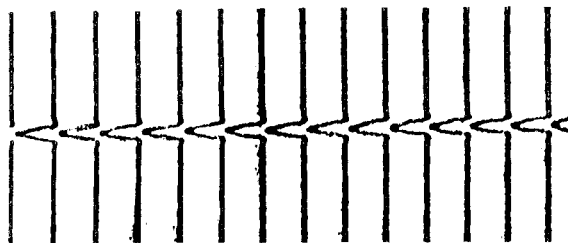


Plate 7 Microinterferogram of multiple-beam Fizeau fringes at reflection of unannealed nylon-6 fiber using monochromatic light of wavelength $\lambda = 546.1$ nm vibrating perpendicular to the fiber axis.

mula for the other direction, n_s^{\perp} and n_c^{\perp} were obtained.

The mean refractive indices of the nylon-6 fiber, n_a^{\parallel} and n_a^{\perp} , were deduced from eq. (2). The obtained refractive indices were used to find values for Δn_s , Δn_c , and Δn_a .

The variations of n_s^{\parallel} , n_c^{\parallel} , n_a^{\parallel} , n_s^{\perp} , n_c^{\perp} , and n_a^{\perp} , as well as of Δn_s , Δn_c , and Δn_a with the different annealing temperatures for the constant annealing time of 3 h are shown in Figure 1. The behavior of n_s^{\parallel} , n_c^{\parallel} , n_a^{\parallel} , n_s^{\perp} , n_c^{\perp} , and n_a^{\perp} as well as of Δn_s , Δn_c , and Δn_a at different annealing temperatures for the constant annealing time of 5 h appears in Figure 2. The change in n_s^{\parallel} , n_c^{\parallel} , n_a^{\parallel} , n_s^{\perp} , n_c^{\perp} , and n_a^{\perp} as well as Δn_s , Δn_c , and Δn_a due to the different intervals of annealing time for the constant annealing temperature of 140°C are depicted in Figure 3.

Multiple-Beam Fizeau Fringes at Reflection for Determining the Mean Refractive Indices and the Mean Birefringence of Nylon-6 Fibers

To confirm the results obtained previously, the multiple-beam Fizeau fringes at reflection method

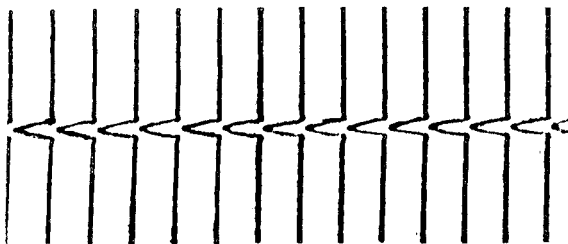


Plate 8 Microinterferogram of multiple-beam Fizeau fringes at reflection of unannealed nylon-6 fiber using monochromatic light of wavelength $\lambda = 546.1$ nm vibrating parallel to the fiber axis.

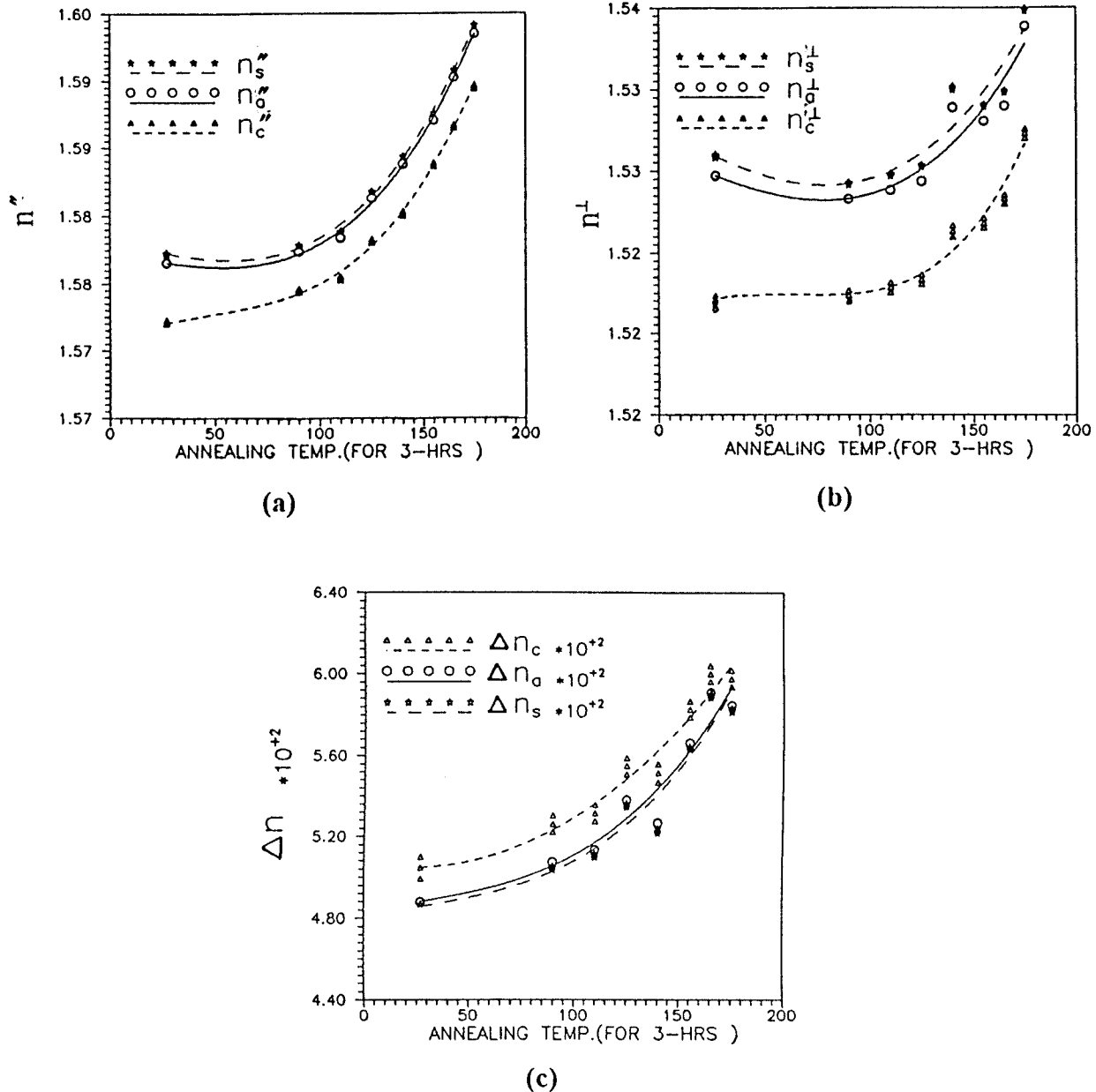


Figure 1 Variation of the refractive indices and birefringence of nylon-6 fiber layers with annealing temperatures for 3 h, measured by multiple-beam Fizeau fringes in transmission: (a) parallel components; (b) perpendicular components; (c) birefringence.

was applied to unannealed nylon-6 fibers. The mean refractive indices n_a^\parallel and n_a^\perp as well as the mean birefringence Δn_a were determined from the fringe patterns.

A microinterferogram of multiple-beam Fizeau fringes at reflection of an unannealed nylon-6 fiber is shown in Plate 7. A monochromatic light of wave-

length 546.1 nm vibrating perpendicular to the fiber axis was used. The refractive index of the used immersion liquid was $n_L = 1.5356$ at 27°C.

Plate 8 is a microinterferogram of multiple-beam Fizeau fringes at reflection of an unannealed nylon-6 fiber. In this case, the monochromatic light of wavelength 546.1 nm was vibrating

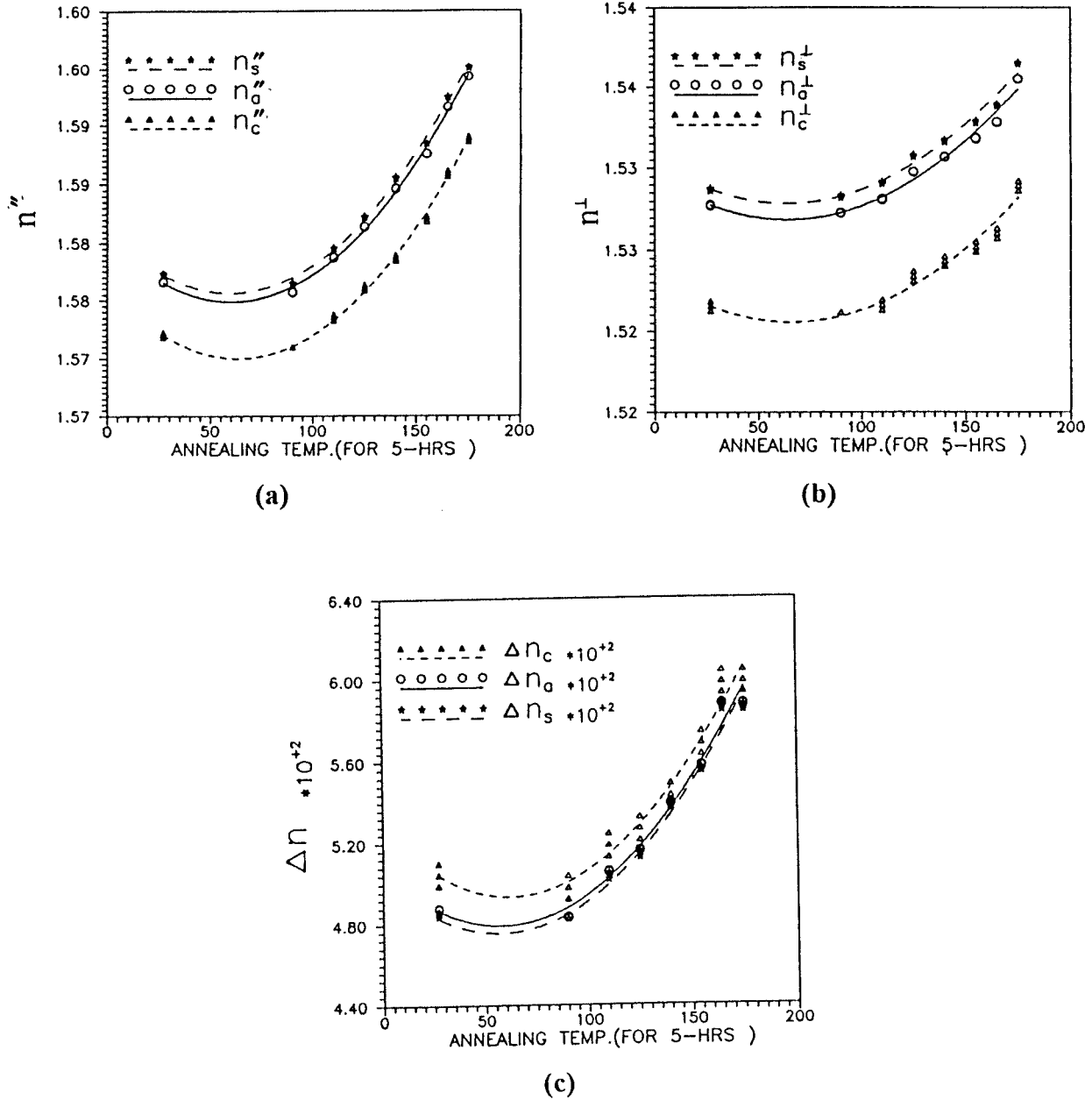


Figure 2 Change in the refractive indices and birefringence of nylon-6 fiber layers vs. annealing temperatures for 5 h, measured by multiple-beam Fizeau fringes in transmission: (a) parallel components; (b) perpendicular components; (c) birefringence.

parallel to the fiber axis and the refractive index of the immersion liquid was $n_L = 1.5845$ at 27°C.

The mean refractive indices and the mean birefringence were calculated by using the following equations¹⁸:

$$n_a^\parallel = n_L + \frac{dz^\parallel}{h} \cdot \frac{\lambda}{2d} \quad (3)$$

with an analogous formula for n_a^\perp , we have

$$n_a^\perp = n_L + \frac{dz^\perp}{h} \cdot \frac{\lambda}{2d} \quad (4)$$

The fringe shift for perpendicular and parallel directions, dz^\perp and dz^\parallel , as well as the interfering

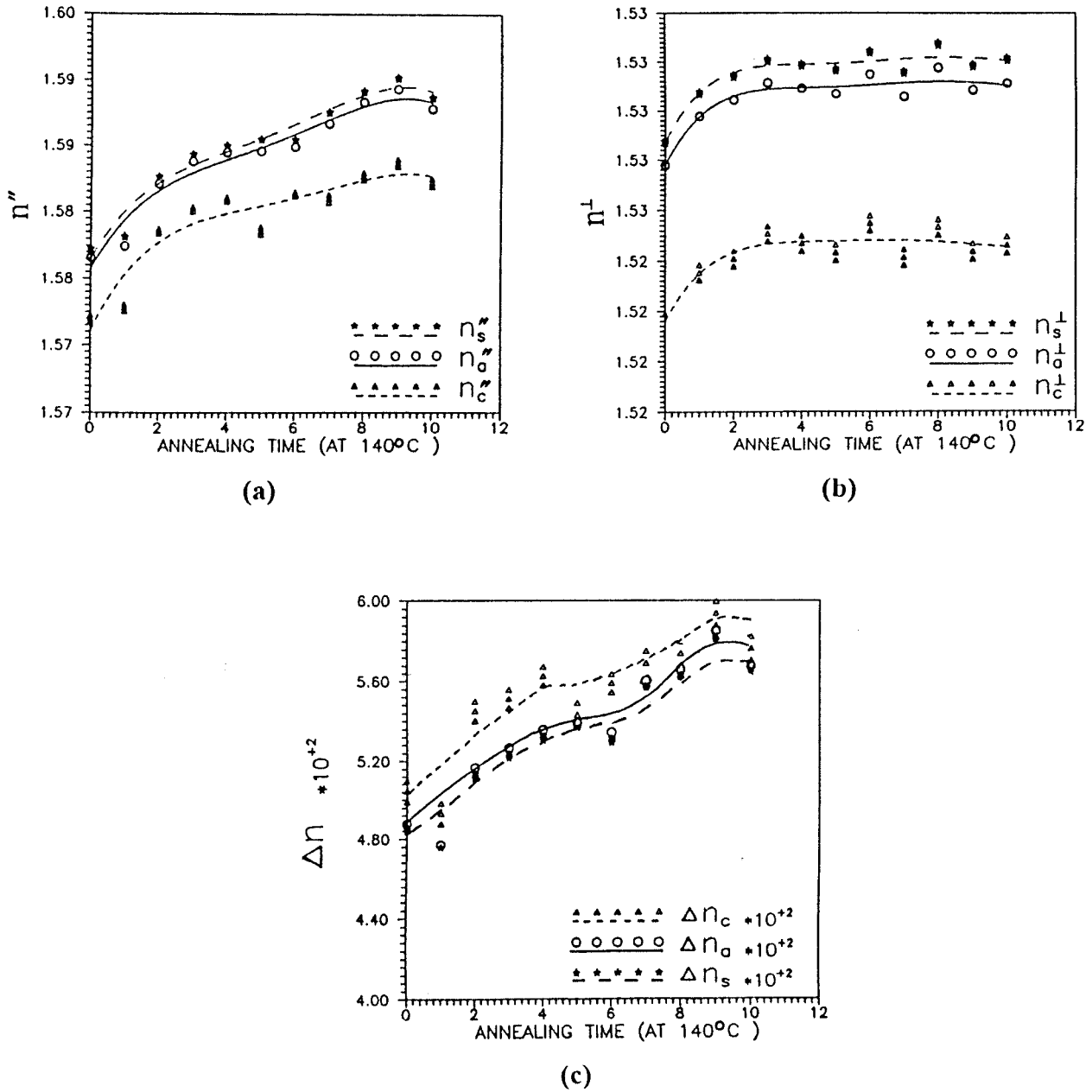


Figure 3 Variation of the refractive indices and birefringence of nylon-6 fiber layers with annealing time at 140°C, measured by multiple-beam Fizeau fringes in transmission: (a) parallel components; (b) perpendicular components; (c) birefringence.

spacing h were determined from the microinterferograms. The fiber thickness d was determined from the microinterferograms and from the obtained optical cross section (Plate 1).

The fringe shift of the fiber in Plates 7 and 8 was found to be away from the apex of the

interferometer. This indicated that, for perpendicular and parallel components, the refractive index of the chosen liquid was higher than that of the fiber.

The calculated mean refractive indices and the mean birefringence are

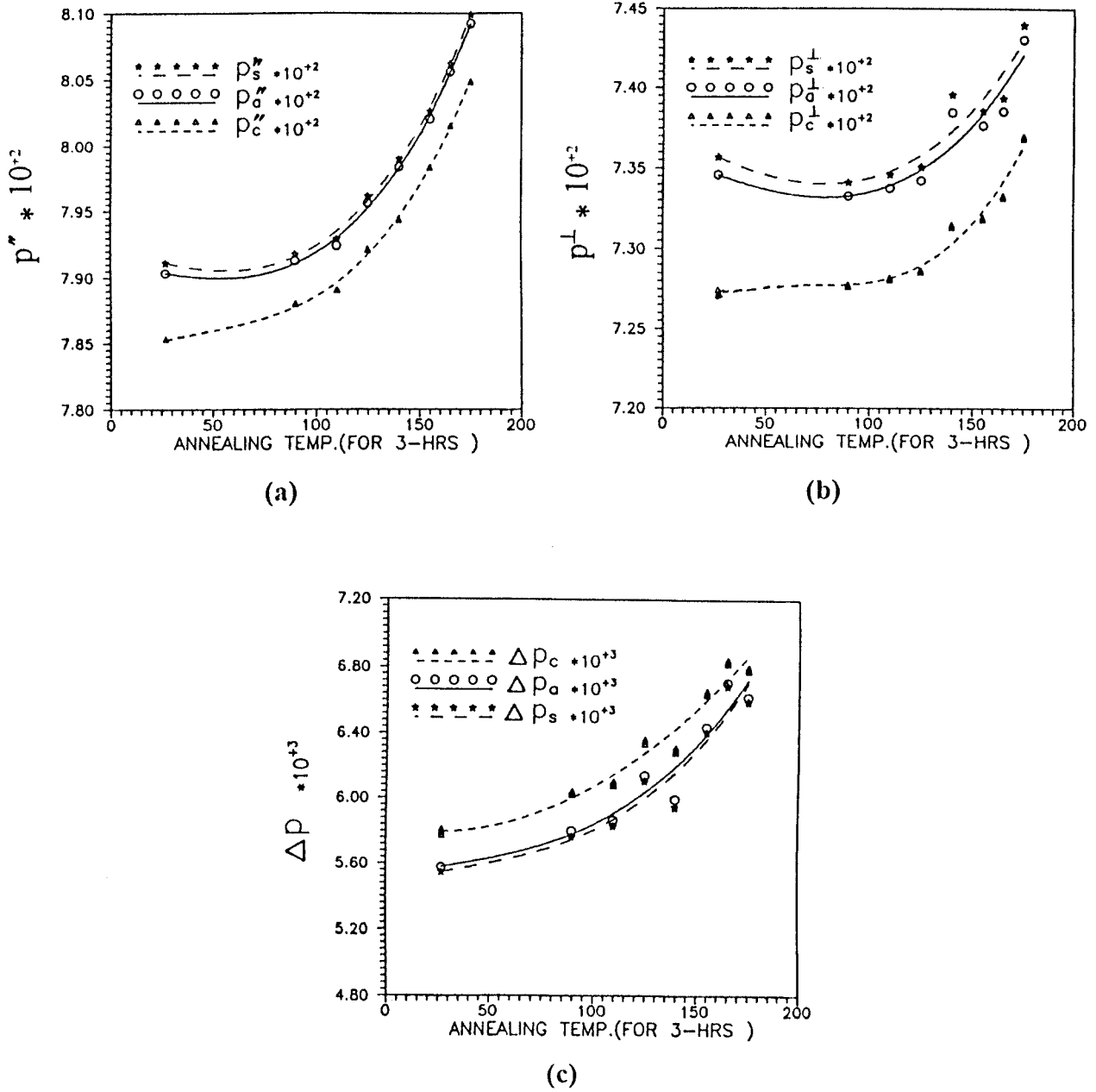


Figure 4 Variation of the polarizabilities per unit volume and ΔP of nylon-6 fiber layers with annealing temperatures for 3 h, measured by multiple-beam Fizeau fringes in transmission: (a) parallel components; (b) perpendicular components; (c) ΔP .

$$n_a^{\parallel} = 1.5766, \quad n_a^{\perp} = 1.5277,$$

$$\text{and } \Delta n_a = 4.9 \times 10^{-2}$$

The application of multiple-beam Fizeau fringes in transmission as well as at reflection did not exhibit significant disagreements.

Determination of the Skin, Core, Mean Polarizabilities per Unit Volume, and Isotropic Refractive Indices of Nylon-6 Fibers

The values for skin and core polarizabilities per unit volume P_s^{\parallel} , P_s^{\perp} , P_c^{\parallel} , and P_c^{\perp} as well as the mean polarizabilities per unit volume P_a^{\parallel} and P_a^{\perp} were calculated from the following equations¹⁹:

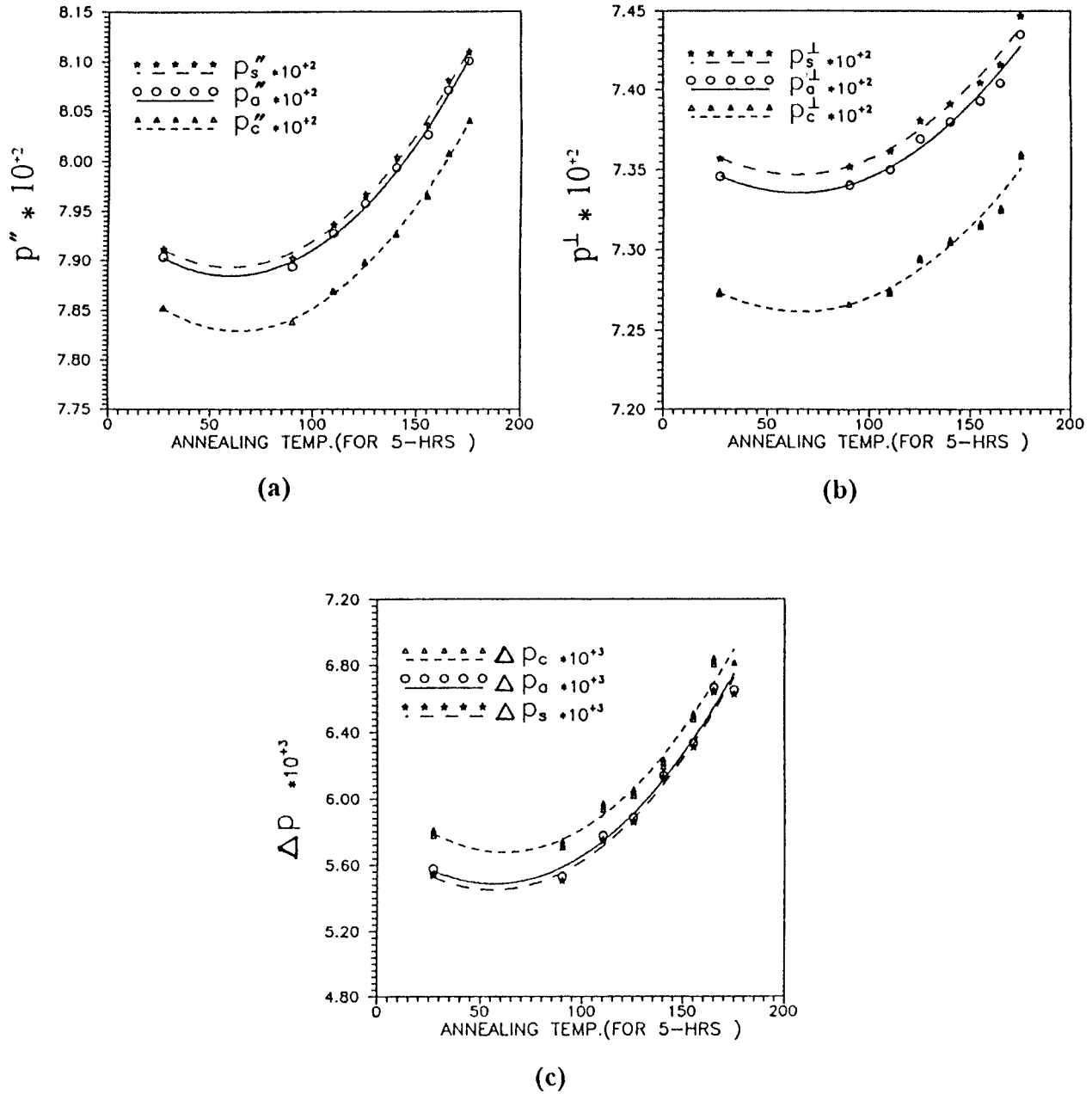


Figure 5 Change in the polarizabilities per unit volume and ΔP of nylon-6 fiber layers vs. annealing temperatures for 5 h, measured by multiple-beam Fizeau fringes in transmission: (a) parallel components; (b) perpendicular components; (c) ΔP .

$$\frac{(n_{\parallel}^2 - 1)}{(n_{\parallel}^2 + 2)} = \left(\frac{4}{3}\right) \pi \cdot P_{\parallel} \quad (5)$$

$$\frac{(n_{\perp}^2 - 1)}{(n_{\perp}^2 + 2)} = \left(\frac{4}{3}\right) \pi \cdot P_{\perp} \quad (6)$$

The calculated skin and core refractive indices along with the mean refractive indices of nylon-6 fibers for plane polarized light, vibrating parallel and perpendicular to the fiber axis, served this purpose. The obtained polarizabilities per unit volume were used to find values for

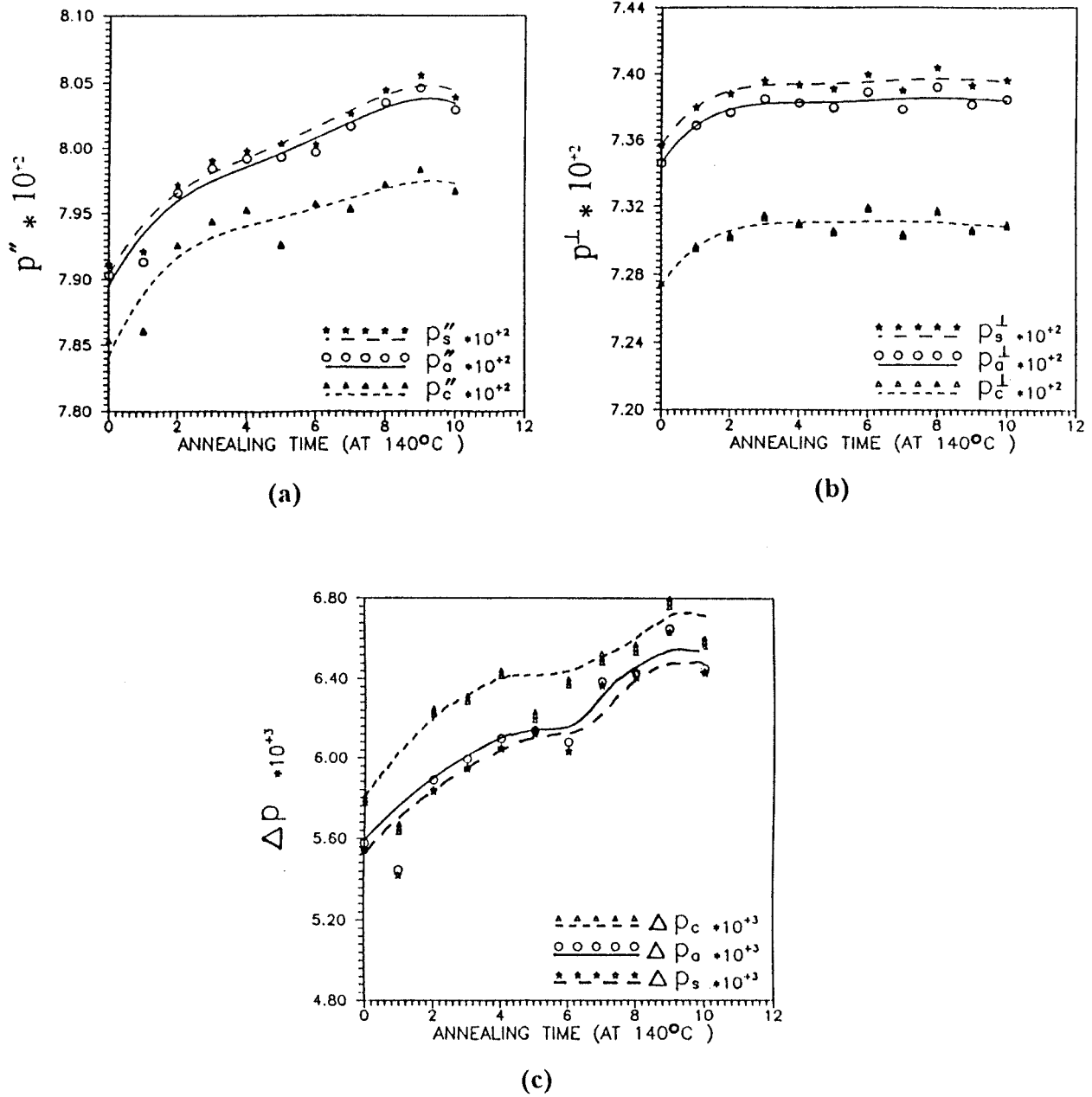


Figure 6 Variation of the polarizabilities per unit volume and ΔP of nylon-6 fiber layers with annealing time at 140°C, measured by multiple-beam Fizeau fringes in transmission: (a) parallel components; (b) perpendicular components; (c) ΔP .

$$\Delta P_s = P_s^{\parallel} - P_s^{\perp}, \quad \Delta P_c = P_c^{\parallel} - P_c^{\perp},$$

$$\text{and } \Delta P_a = P_a^{\parallel} - P_a^{\perp}$$

With the aid of the following equation²⁰:

$$n_{\text{iso}} = \frac{1}{3}[n_a^{\parallel} + 2n_a^{\perp}] \quad (7)$$

the obtained values of the skin, core, and mean refractive indices using multiple-beam Fizeau fringes were used to determine the skin, core, and mean isotropic refractive indices $n_{\text{iso-s}}$, $n_{\text{iso-c}}$, and $n_{\text{iso-a}}$, respectively.

The variations of P_s^{\parallel} , P_c^{\parallel} , P_a^{\parallel} , P_s^{\perp} , P_c^{\perp} , and P_a^{\perp} as well as of ΔP_s , ΔP_c , and ΔP_a with different anneal-

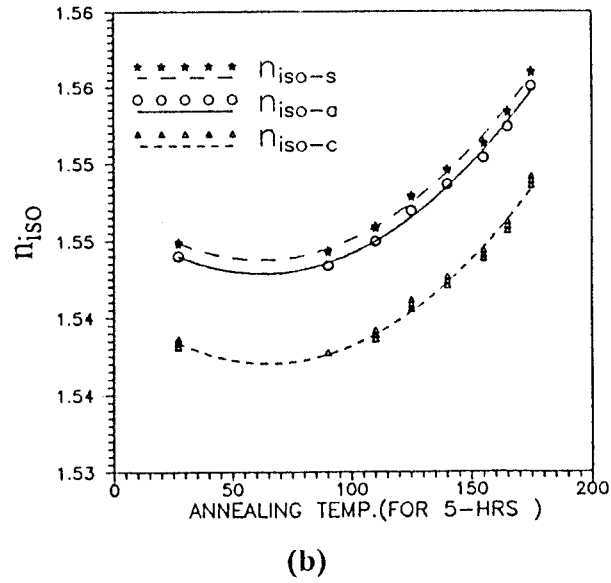
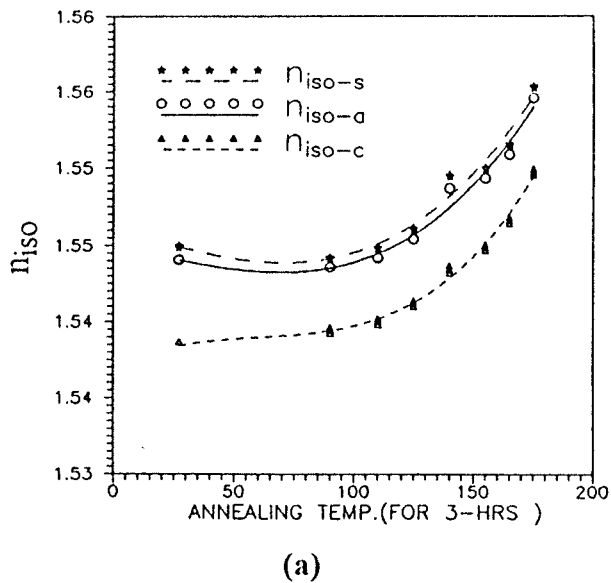


Figure 7 Variation of the isotropic refractive indices of nylon-6 fiber layers vs. the annealing temperatures by multiple-beam Fizeau fringes in transmission: (a) for 3 h; (b) for 5 h.

ing temperatures at the constant annealing time of 3 h are shown in Figure 4. The behavior of P_s^{\parallel} , P_c^{\parallel} , P_a^{\parallel} , P_s^{\perp} , P_c^{\perp} , and P_a^{\perp} as well as of ΔP_s , ΔP_c , and ΔP_a at different annealing temperatures for the constant annealing time of 5 h appears in Figure

5. The changes in P_s^{\parallel} , P_c^{\parallel} , P_a^{\parallel} , P_s^{\perp} , P_c^{\perp} , and P_a^{\perp} as well as in ΔP_s , ΔP_c , and ΔP_a due to the different intervals of annealing time for the constant annealing temperature of 140°C are depicted in Figure 6.

The variations of n_{iso-s} , n_{iso-c} , and n_{iso-a} with the different annealing temperatures at the constant

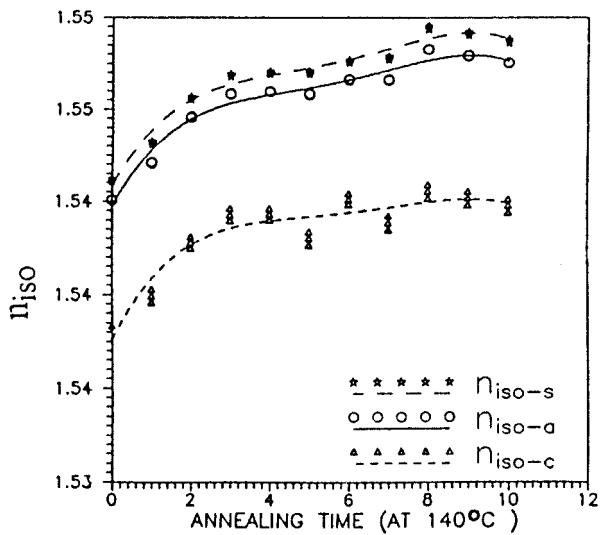


Figure 8 Relation between the isotropic refractive indices of nylon-6 fiber layers and the annealing time at 140°C by multiple-beam Fizeau fringes in transmission.

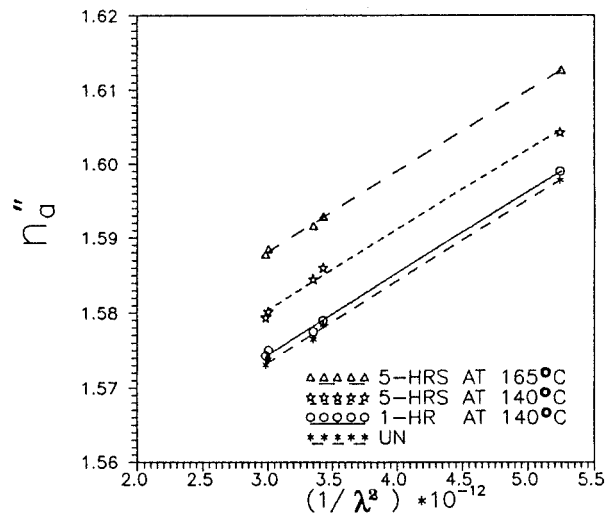


Figure 9 Variation of n_{\parallel} of nylon-6 fibers unannealed and annealed for 1 h at 140°C and for 5 h at 140 and 165°C with $(1/\lambda^2)$.

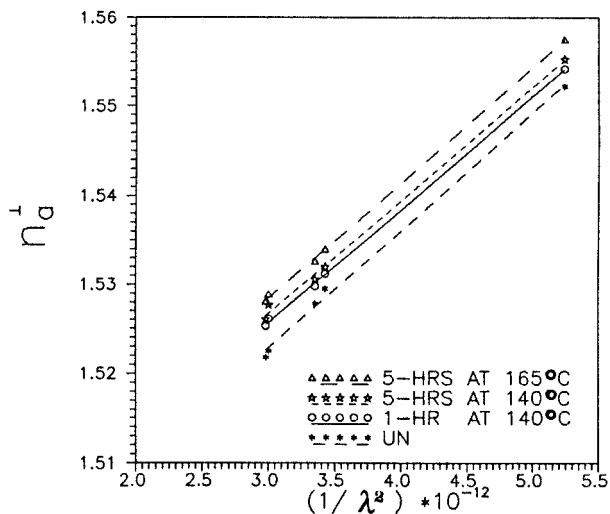


Figure 10 Variation of n_a^\perp of nylon-6 fibers unannealed and annealed for 1 h at 140°C and for 5 h at 140 and 165°C with $(1/\lambda^2)$.

annealing time of 3 and 5 h are shown in Figure 7. The changes in n_{iso-s} , n_{iso-c} , and n_{iso-a} corresponding to the different intervals of annealing time for the constant annealing temperature of 140°C appear in Figure 8.

Application of Multiple-Beam Fizeau Fringes for Calculating the Constants of Cauchy’s Dispersion Formula for Nylon-6 Fibers

Multiple-beam Fizeau fringes in transmission was used for determining the mean refractive indices n_a^\parallel and n_a^\perp for an unannealed nylon-6 fibers and for some samples annealed at different conditions using eqs. (3) and (4). The relation between the mean refractive indices of nylon-6 fibers unannealed and annealed for 1 h at 140°C and for 5 h at 140 and 165°C vs. $(1/\lambda^2)$ for light vibrating parallel and perpendicular to the fiber axis are represented in Figures 9 and 10, respectively.

The straight lines of Figures 9 and 10 verify the well-known Cauchy’s dispersion formula

$$n_a = A + \left(\frac{B}{\lambda^2} \right)$$

From these figures, the constants A and B of Cauchy’s dispersion formula are given in Table I after using the least-squares fitting method.

DISCUSSION

From the previous data and the corresponding figures obtained in this work, several remarks can be made: The variation in n_s^\parallel , n_c^\parallel , and n_a^\parallel as well as in P_s^\parallel , P_c^\parallel , and P_a^\parallel , during the thermal treatment, is greater than in n_s^\perp , n_c^\perp , n_a^\perp , P_s^\perp , P_c^\perp , and P_a^\perp , although the general trend is almost similar. This indicates that the reorientation of nylon-6 fibers is stronger in the parallel direction than in the perpendicular direction, i.e., Δn_s , Δn_c , and Δn_a as well as ΔP_s , ΔP_c , and ΔP_a are positive.

At the constant temperature of 140°C, for the first 2 h of annealing, n_s^\parallel , n_s^\perp , Δn_s , n_c^\parallel , n_c^\perp , Δn_c , n_a^\parallel , n_a^\perp , and Δn_a as well as P_s^\parallel , P_s^\perp , ΔP_s , P_c^\parallel , P_c^\perp , ΔP_c , P_a^\parallel , P_a^\perp , ΔP_a , n_{iso-s} , n_{iso-c} , and n_{iso-a} exhibited the same linear behavior. Between 2 and 8 h of annealing at the annealing temperature of 140°C, the change in the above parameters was considerably small. This probably indicates an adaptation of the macromolecular structure of nylon-6 fibers to the ambient temperature.

At constant annealing time durations of 3 and 5 h, while increasing the temperature from 90 to 175°C, the behavior of the layers and the mean refractive indices, birefringence, polarizabilities per unit volume, and isotropic refractive indices approximately agreed with the exponential behavior in its increase. Between 27 and 110°C, the

Table I Values of Cauchy’s Dispersion Formula Constants for Unannealed and Annealed Nylon-6 Fibers at Different Conditions

Nylon-6 Samples	A^\parallel	A^\perp	$B^\parallel \times 10^{-15} \text{ m}^2$	$B^\perp \times 10^{-15} \text{ m}^2$
Unannealed	1.5407	1.4831	10.89	13.24
Annealed for 1 h at 140°C	1.5416	1.4875	10.93	12.72
Annealed for 5 h at 140°C	1.5481	1.4885	10.78	12.73
Annealed for 5 h at 165°C	1.5554	1.4896	10.91	12.96

changes in the refractive indices, the birefringence, and, hence, the polarizabilities were considerably small.

The linear increase that followed, at the temperature range 125–175°C, indicates that the structure of the fiber was drastically affected. A general deduction from the figures of the present work is that the fiber was affected by isothermal annealing, keeping $n_c < n_a < n_s$ for both the parallel along and across the fiber axis.

It was observed visually that the color of the nylon-6 fibers suffered an unnoticeable change when the annealing temperature range was 90–125°C, although the time duration reached 10 h. On the other hand, when annealing took place at high temperatures (140–175°C), a variation in the color accompanied the increase of annealing time duration. The hue changed between light to dark ivory in this range of temperatures.

CONCLUSION

From the above discussion and considerations, the following conclusions may be drawn:

1. The multiple-beam Fizeau fringes method showed that the fiber surface (skin) has a different effect from that of its core. The microinterferograms clearly identify these differences in optical path variations. The results may be used for monitoring the isothermal process of these polymer fibers.
2. The refractive indices' measurements indicated that the structure of the fiber along its axis is different from that across its axis, which was expected due to the anisotropic phenomena for these fibers.
3. The annealing process affects other physical properties (swelling,²¹ dyeability, electrical, dielectric, color,⁹ mechanical,²² etc.) which needs further studies to detect which properties are improved by annealing for nylon-6 fibers.
4. The use of multiple-beam Fizeau fringes verified the Cauchy's dispersion formula and determined its constants A and B . In Table I, the changes of these constants for unannealed and annealed nylon-6 fibers at different conditions were shown.
5. As there are variations in the density due to the change in n_{iso} , so also the crystallin-

ity and crystalline parameters of the fiber material varied systematically with different annealing conditions.

6. There are visual color changes for nylon-6 fibers due to different annealing conditions in the air.

We conclude from the above results and considerations that the practical importance of these measurements provides acceptable results for the optothermal parameters. Since n_s^{\parallel} , n_s^{\perp} , n_c^{\parallel} , n_c^{\perp} , n_a^{\parallel} , n_a^{\perp} , . . . , etc. are a consequence of the material annealed, so reorientation of nylon-6 fibers may occur not only during manufacture but also due to the annealing process. Also, it is acceptable that the multiple-beam technique is very promising to reveal the changes due to the annealing process for the optical behavior of the skin–core structure of nylon-6 fibers.

The authors thank Prof. Dr. Abdel Hady Saleh of the Physics Department, Faculty of Science, Cairo University, for his useful discussions.

REFERENCES

1. A. A. Hamza, I. M. Fouda, K. A. El-Farahaty, and E. A. Seisa, *Polym. Test.*, **10**, 83–90 (1991).
2. R. J. Samuels, *Structured Polymer Properties*, Wiley, New York, London, 1974, pp. 51–63.
3. A. A. Hamza, I. M. Fouda, T. Z. N. Sokkar, M. M. Shahin, and E. A. Seisa, *Polym. Test.*, **11**, 297 (1992).
4. I. M. Fouda and M. M. El-Tonsy, *J. Mater. Sci.*, **25**, 121 (1990).
5. I. M. Fouda and M. M. El-Tonsy, *J. Mater. Sci.*, **25**, 4752–4757 (1990).
6. I. M. Fouda, M. M. El-Tonsy, and M. A. Shaban, *J. Mater. Sci.*, **26**, 5085–5092 (1991).
7. A. A. Hamza, I. M. Fouda, M. M. El-Tonsy, and F. M. El-Sharkawy, *J. Appl. Polym. Sci.*, **56**, 1355 (1995).
8. I. M. Fouda, M. M. El-Tonsy, and H. M. Hosny, *Polym. Degrad. Stab.*, **46**, 287 (1994).
9. A. A. Hamza, M. M. El-Tonsy, I. M. Fouda, and A. M. El-Said, *J. Appl. Polym. Sci.*, **57**, 265–270 (1995).
10. O. W. Statton, *J. Polym. Sci. Part A2*, **10**, 1587 (1972).
11. E. A. Zachariades and S. R. Porter, *The Strength and Stiffness of Polymers*, Marcel Dekker, New York, Basel, 1983, p. 121.

12. F. Decandai and Vittoria, *J. Polym. Sci. Phys. Ed.*, **23**, 1217 (1985).
13. G. William, P. Perkins, and S. R. Porter, *J. Mater. Sci.*, 2355 (1977).
14. W. Haward, J. R. Starkweather, E. M. George, J. E. Hansen, T. M. Roder, and R. E. Brooks, *J. Polym. Sci.*, **21**, 201 (1956).
15. A. A. Hamaza, I. M. Fouda, T. Z. N. Sokker, and M. A. El-Bakary, *Polym. Int.*, to appear.
16. M. M. El-Nicklaway and I. M. Fouda, *J. Text. Inst.*, **71**, 252–256 (1980).
17. N. Barakat, *Text. Res. J.*, **41**, 167–170 (1971).
18. N. Barakat and A. M. Hindeleh, *Text. Res. J.*, **34**, 357–362 (1964).
19. I. M. Ward, *Structure and Properties of Oriented Polymers*, Applied Science, London, 1975, p. 57.
20. H. Hannes, *Kolloid Z. Z. Polym.*, **250**, 765–774 (1972).
21. I. M. Fouda, M. M. El-Nicklaway, E. M. Naser, and R. M. El-Agamy, *J. Appl. Polym. Sci.*, **66**, 1247–1267 (1996).
22. A. A. Hamza, I. M. Fouda, M. M. Kabeel, and H. M. Shabana, *Polym. Test.*, **10**, 305 (1991).